Journal of Statistical Physics, Vol. 60, Nos. 3/4, 1990

Current Distribution on a Three-Dimensional, Bond-Diluted, Random-Resistor Network at the Percolation Threshold

Edgardo Duering[1-3] and David J. Bergman[2]

Received July 25, 1989; final February 23, 1990

Current and logarithm-current distributions on a three-dimensional random-bond percolation cubic network were studied at the percolation threshold by computer simulations. Predictions of a hierarchical model that combine fractal structure and randomness agree with our numerical simulations. In the thermodynamic limit the logarithm-current distribution exhibits an $n(\ln(i)) \sim i^{1/3}$ dependence below some characteristic current i_c. This distribution may scale with $\ln i/\ln L$, but the data are insufficient to make this a definite conclusion. Due to the small range of $\ln L$ considered, a study of the moments does not reveal this behavior and a study of the distribution itself is required.

KEY WORDS: Percolation; multifractals; transport processes; distribution.

1. INTRODUCTION

The critical behavior of self-similar resistor networks is characterized by an infinite set of exponents.[1-5] Standard exponents such as the fractal dimension, the resistance exponent, and the correlation length exponent in percolation are members of this set. The term *multifractal* has been coined to describe a physical or geometric object that requires such an infinite set of independent exponents to characterize its properties. In the context of resistor networks the multifractal character has been related to the asymptotic shape of the current distribution.[3] More precisely, each moment of the current distribution is characterized by a different exponent.

[1] School of Physics and Astronomy, Raymond and Beverly Sackler Faculty of Exact Sciences, Tel Aviv University, Tel Aviv 69978, Israel.
[2] Department of Chemical Physics, Weizmann Institute of Science, Rehovot 76100, Israel.
[3] Current address: Max Planck Institut für Polymerforschung, D-6500 Mainz, FRG.

0022-4715/90/0800-0363$06.00/0

A comprehensive study of the properties of this set of exponents was presented by Blumenfeld *et al.*[5] Consider a two-terminal measurement on an arbitrary fixed cluster in which a unit current I is injected at a source site x and removed at a sink site x'. This imposed current will give rise to a distribution of currents in bonds covering a region associated with x and x'. A simple way of characterizing this distribution involves its moments,[3]

$$M_q(x, x') = \sum_b |I_b|^q \tag{1.1}$$

where we sum over all bonds b which carry a nonzero current I_b. This current implicitly depends on x and x'.

Critical exponents can be defined in association with each moment via

$$M'_q = [v(x, x')\, M_q(x, x')]_{\mathrm{av}}/[v(x, x')]_{\mathrm{av}} \sim |x - x'|^{x_q}, \qquad 1 \ll |x - x'| \ll \xi \tag{1.2}$$

where ξ is the percolation correlation length, and $v(x, x')$ is the indicator function for percolation: i.e., it is one if sites x and x' are in the same cluster and zero otherwise; $[\cdot]_{\mathrm{av}}$ indicates an average over all configurations of occupied and unoccupied bonds and[1,5,6] $x_q = \psi_q/\nu$. Note that our symbol x_q differs in sign from the one used in ref. 1, i.e., our x_{2q} is the same as $-x_q$ of that reference. Then we can study the moments of the current distribution as a function of the linear dimension $R = |x - x'|$ that we can write as $A_q R^{x_q}$. If instead of a unit current we apply a unit voltage, the corresponding moments scale as

$$M_q = A'_q R^{x'_q} \tag{1.3}$$

with $x'_q = x_q - q x_2$ and by definition the amplitudes A'_q and A_q are independent of R and they are in general a smooth function of q.

The ratio $b = x_1/x_2$ for percolating systems in three dimensions ($d = 3$) is known from recent numerical simulations on continuum systems composed of intersecting spheres[7] [$\kappa = \nu(d - b) = 1.57 \pm 0.08$] and on random resistor networks[8] ($\kappa = 1.47 \pm 0.04$, $b = 1.35 \pm 0.04$). Series expansions[5] and ε-expansion[6] results also exist, as well as exact bounds on b[9,10]: $1.21 \pm 0.06 \leqslant b \leqslant 1.30 \pm 0.13$. The positive moments of the logarithm-current distribution, on a class of hierarchical structures that combine randomness of the structure with features of the exact fractal, were shown to scale as function of the linear dimension of the system[11]

$$m_q = \sum_b \ln^q I_b = B_q R^{D_B} \ln^{\beta(q)} R \tag{1.4}$$

where $N_{BB} = R^{D_B}$ is the number of bonds on the backbone connecting x

and x' and D_B is the backbone dimension. The ratio m_q/N_{BB} is thus a function of R,[11]

$$\mathscr{M}_q = \frac{m_q}{N_{BB}} = B_q \ln^{\beta(q)} R \tag{1.5}$$

where, for the above mentioned hierarchical structures,

$$\beta(q) = cq \tag{1.6}$$

and where, by definition, the amplitude B_q is independent of R but could be a function of q. Based on those studies, c is predicted to be one, in any dimension. For negative values of q, these asymptotic scaling forms may have to be corrected for finite size effects when $-q > \ln R$. Consequently, in our analysis of the negative moments we assumed the modified scaling forms.[11]

$$m_{-q} = R^{D_B+\delta} \ln^{-c'q} R \tag{1.7}$$

$$\mathscr{M}_{-q} = \frac{m_{-q}}{N_{BB}} = R^{\delta} \ln^{-c'q} R \tag{1.8}$$

where c' may differ from c of (1.6), and where the exponent δ was sometimes allowed to be nonzero. All of these scaling forms are believed to remain unchanged if, instead of applying a unit potential difference, we apply a unit current to the system.

While the scaling predictions of the moments of the current distribution are satisfied for large, positive values of q, they fail for sufficiently large negative q values, where the dominant small currents decrease exponentially with size. There are indications[12] that for these small currents the roundoff errors of numerical simulations are important and could strongly affect the results. The roundoff error effect is also important when we calculate the positive moments of the logarithm-current distributions, since the small currents then play a dominant role, too.

The transfer matrix method of ref. 12 seems to be especially suited for a careful study of these distributions. The main objective of this paper is to present a clear discussion of the method we applied to study the logarithm-current distribution. Special attention was given to the roundoff error problem and to a discussion of finite-size scaling properties.

It was found that the distribution of currents in a random resistor network is not a scaling function of a variable like (i/R^a).[1,3,5,13,14] Later it was claimed that this distribution tends to a log-normal form for very

large systems.[3] This was also shown to be incorrect by simulations of two-dimensional networks.[15] As was concluded in that reference, we too find that the function $n(\ln(i))$ has a very simple asymptotic form for small i. We find that

$$n(\ln(i)) \sim i^{\gamma(L)} \tag{1.9}$$

for $i < i_c$, where i_c is a characteristic upper cutoff, L is the linear size of the network and $\gamma(L)$ is an L-dependent exponent. For example, when $L = 18$, the logarithm of this distribution $\ln[n(\ln(i))]$ increases linearly with $\ln(i)$ over about five orders of magnitude of i, limited only by roundoff errors.

2. THE NETWORK MODEL AND ITS NUMERICAL SIMULATION

The random-resistor bond percolating cubic network consists of a number $N\ (=L+1)$ of x–y planes connected through bonds oriented along the z direction (see Fig. 1a). Each plane contains L^2 sites that can be either connected to the faces A and B and disconnected from the faces C and D, or connected to C and D and disconnected from A and B. The sites are never simultaneously connected to all faces A, B, C, and D. When all bonds are present, their total number is $2L(L+1)^2 + L^3$. In its randomly diluted version, this type of network allows us to obtain the current distribution when a potential difference is applied either along the y direction, between faces A and B, or along the x direction, between faces C and D.

A cluster of bonds that connect faces A and B is a percolating cluster in the y direction, while a cluster that connects faces C and D is a percolating cluster in the x direction. Only those networks that percolate in both directions were considered. The reasons for this, as well as the somewhat odd form of the networks that we used, have to do with the original purpose for which these networks were simulated, namely, a study of the Hall effect at the percolation threshold. The present study uses the same data that was generated in those simulations. That study was described elsewhere,[12] along with a detailed description of the modified transfer-matrix method which we developed for calculating the voltages on all bonds of the network. Here we only give a brief summary of that method.

A potential difference of 1 was applied between a pair of parallel faces. Note that this is different from the conditions assumed to obtain Eq. (1.5): In that case the potential difference was applied between a pair of points at x and x'. We assume that Eq. (1.5) continues to hold for our case, too.

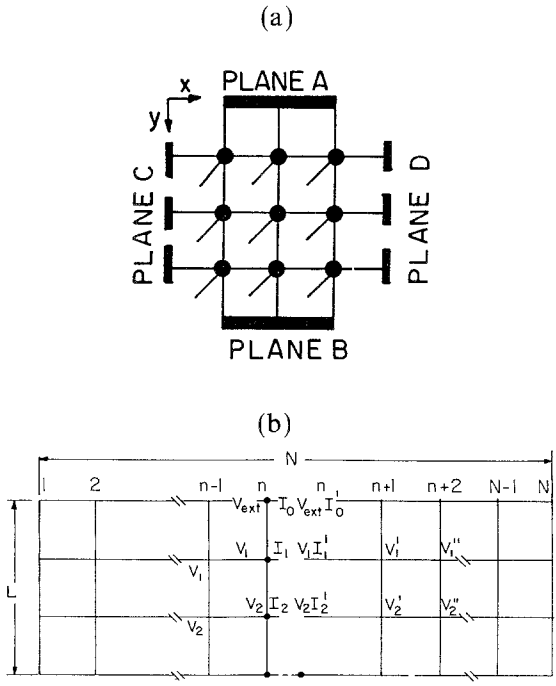

Fig. 1. (a) A single x, y layer of the network model used in the simulations with $L=3$. We observe the $L^2=9$ sites, as well as the $L(L+1)=12$ unit cells in the x and in y directions. Here A and B are the pair of faces between which a potential difference is being applied, while at the other pair of faces C, D a zero-current boundary condition is imposed. When the faces A and B were connected, the faces C and D were disconnected, and vice versa. (b) 2D strip network split up at the nth layer into left and right subnetworks on which we describe the transfer matrix method explained in the text. See ref. 12 for further details.

Each bond of the network has an Ohmic conductivity $\sigma=1$ with probability p_c, and $\sigma=0$ with probability $(1-p_c)$, where the percolation threshold value p_c was taken to depend on the linear size L according to[16]

$$p_c(L) = -0.2492 + 0.071L^{-1/0.88} + 1.25L^{-2/0.88} \tag{2.1}$$

The method of ref. 13 was applied to obtain the currents in all bonds of the network. In this method an admittance matrix A_{ij}^L is constructed for each x–y section of the network (see Fig. 1b), starting from $A_{ij}^L=0$ at the $z=0$ plane.[17] Another admittance matrix A_{ij}^R is constructed for the same section, starting from $A_{ij}^R=0$ at the $z=N$ plane. For a given section at $z=z_0$, the A^L matrix characterizes the response of the network to the left

of z_0 by relating the currents I_i to the voltages V_j externally applied at each site of the section

$$I_i = \sum_j A_{ij}^L V_j \tag{2.2}$$

The other matrix A^R similarly characterizes the response of the network to the right of z_0,

$$I_i' = \sum_j A_{ij}^R V_j' \tag{2.3}$$

The two sets of equations are combined into one set of equations for V_j by noting that in the combined network we must have $V_j = V_j'$ at all sites and $I_i + I_i' = 0$ at all internal sites, while $I_i + I_i' = I_{\text{ext}}$ for the sites representing the external connections.

3. COLLECTING THE RELEVANT INFORMATION

During the analysis of the logarithm-current distribution it is very important to carefully eliminate roundoff errors, since the smallest currents i give the largest values of $\ln(i)$.

As can be seen from Figs. 2a and 2b for $L = 18$, for large values of L ($L > 10$) some very small currents appear that cannot be distinguished from those spurious currents that appear as a result of roundoff error, in bonds where the current should vanish (e.g., in dangling clusters). Figure 2b is particularly instructive in this respect.

It was therefore very important to carefully select an L-dependent value of the minimum current that can be considered as a true current rather than a roundoff error. This value, which we denote by ε, can only be determined after the collection of some data, by considering a plot such as Fig. 2b. We therefore proceeded as follows: We first selected two particular values $i_{\min}$ and $i_{\max}$ (we will see later how to choose them) such that $i_{\min} \sim \varepsilon$ and $i_{\max} > \max(\sigma_e)$, with $\max(\sigma_e)$ as the estimated maximum effective conductivity possible in any system of linear dimension L. Potential differences $V_{AB} = V_{CD} = 1$ were chosen as boundary conditions. Since the current in any bond falls between $i_{\min}$ and $i_{\max}$, this interval was divided into N equally spaced bins ($N = 2000$) in which we simply accumulated bond numbers. In this way we could store the approximate current distribution of $\mathcal{N}$ systems of linear dimension L in just one vector of length N.

The values of $i_{\min}$ and $i_{\max}$ were chosen from the analysis of preliminary results. In order to collect these results, we need some estimate of $i_{\min}$ and $i_{\max}$. From the analysis of the data of ref. 12 we know that $i_{\min}$ will be close to but greater than 10^{-12}, while $i_{\max} \leqslant 1$. We therefore chose $i_{\min} = 10^{-12}$ and $i_{\max} = 1$ for storing the preliminary results. From these data, better values $i_{\min}$ and $i_{\max}$ were obtained, which were then similarly used in accumulating the rest of the data. Figure 2c exhibits an implementation of this for a special case.

In later calculations the Hoshen–Kopelman algorithm[18] used in these simulations to eliminate finite clusters was replaced by the burning method,[19] which eliminates also all the dangling clusters. The implementation of burning, before applying the transfer matrix method to calculate the current distributions, eliminated the spurious currents which appeared when the Hoshen–Kopelman algorithm was used. This shows that those currents were indeed unphysical currents which appeared in the dangling ends.

In a similar fashion we saved the logarithm-current distribution in $N = 2000$ bins equally spaced between $\ln(i_{\min})$ and $\ln(i_{\max})$. Figures 2a and 2b exhibit an implementation of this for a special case.

This procedure for data storage using N bins ($N = 2000$) means that we stored the distribution function to only three significant digits. This was accurate enough to obtain the moments of the distribution. As we have smooth distributions, it turns out that the results are even better that what might have been expected.

Obviously we could also obtain the current distribution from the logarithm-current distribution and this was done to check how sensitive our results are to the method of data storage (or size of the bins). This and other checks showed that the error originating from our finite resolution or finite bin size is smaller than the random statistical errors and can be neglected.

As we pointed out previously, the distribution moments were obtained after the collection of all the data in order to avoid the roundoff error effects. However, in order to calculate the statistical errors, we need to know these moments for indificual samples. Since the currents from different samples with the same L were stored in a single array of bins, this information was not available during the analysis of the corrected distributions. To obtain an estimate of the statistical errors, the moments of the distributions were evaluated for each sample during the collection of the data, before the distribution could be corrected for roundoff errors. Then their mean values and statistical errors were calculated. At the lower values of L, where the roundoff errors were small, those initially calculated mean values were in good agreement with the final values. This agreement

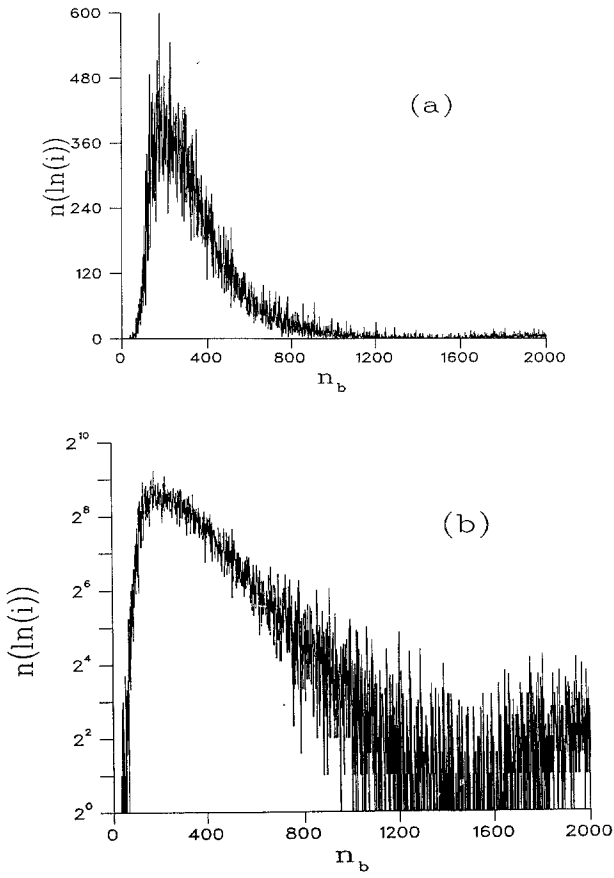

Fig. 2. (a) Logarithm-current distribution $n(\ln(i))$ versus the bin number $n_b = k \ln(i/i_{\max})$ with $k = 2000/\ln(i_{\min}/i_{\max})$, $i_{\min} = 10^{-10}$, and $i_{\max} = 0.09$, for $L = 18$. (b) Logarithm of the logarithm-current distribution $\ln[n(\ln(i))]$ versus the bin number n_b for $L = 18$ and the same n_b definition as in (a). (c) Current distribution $n(i)$ versus the bin number $n_b = ki$ with $k = 2000/i_{\max}$ with $i_{\max} = 0.09$ for $L = 18$ and $i_{\max} = 0.17$ for $L = 10$.

deteriorates at the larger L values. We can infer from this that at the lower L values the calculated statistical errors are also substantially without roundoff error effects. For larger L values the calculated statistical error increases, but this is probably due mostly to the increase in the roundoff error effect. At the largest values of L ($L \geqslant 16$) the uncorrected errors we estimated were very large. We quote the corrected mean values without being able to estimate the errors, other than to say that those should be quite small (see Figs. 4a and 4b below).

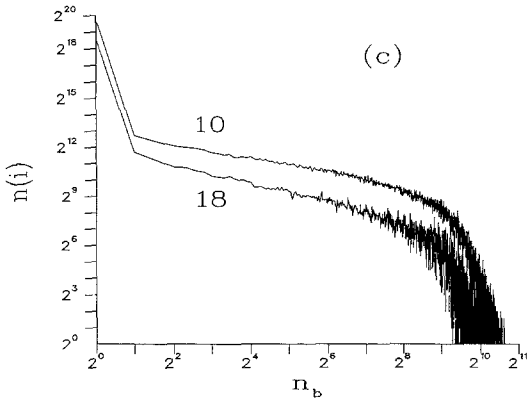

Fig. 2. (*Contnued*)

4. CHOICE OF A LINEAR SIZE

In the literature the assignment of the characteristic linear dimension of the system is not unique. Different authors chose different ways to define the characteristic linear dimension and this has led to different values for the same exponents and to difficulties in comparing values of exponents obtained in different calculations. Jerauld *et al.*[20] chose the cube root of the number of sites in the network, Herrmann *et al.*[19] chose the edge length, and Derrida *et al.*[21] chose the linear dimension so that a homogeneous network ($p = 1$) would have the same conductivity as a cube of edge length L. For the present case it could be argued that the moments should be studied as a function of the distance between parallel faces A and B or C and D ($L+1$ in bond units) (see Section 3).

It could be also argued that we should use

$$L = \frac{\text{cross-sectional area}}{\text{distance between opposite faces}} \tag{4.1}$$

or

$$\mathscr{L} = (\text{volume})^{1/3} \tag{4.2}$$

As L goes to infinity, the results should be independent of the particular definition used for the linear dimension of the system, but for the range of L values $7 \leqslant L \leqslant 24$ that we considered, the results could depend on this definition. Special attention is given to this question when it arises.

5. RESULTS OF CURRENT AND LOGARITHM-CURRENT DISTRIBUTIONS

In Fig. 2b we exhibit the logarithm-current distribution $n(\ln(i))$ as a function of the bin number $n_b = k \ln(i/i_{\max})$ with $k = 2000/\ln(i_{\min}/i_{\max})$, $i_{\min} = 10^{-10}$, and $i_{\max} = 0.09$, for $L = 18$. Three regions can clearly be distinguished in this graph: a region with $n_b > 1500$ where mainly roundoff errors are observed, a narrow region of relatively high currents, and a wider region of small currents in which the logarithm of $n(\ln(i))$ varies linearly as a function of $k \ln(i/i_{\max})$ over five decades of i. For $10^{-8} < i < 4 \cdot 10^{-3}$ and $L = 18$ we obtain

$$n(\ln(i), L = 18) = i^{0.50 \pm 0.02} \tag{5.1}$$

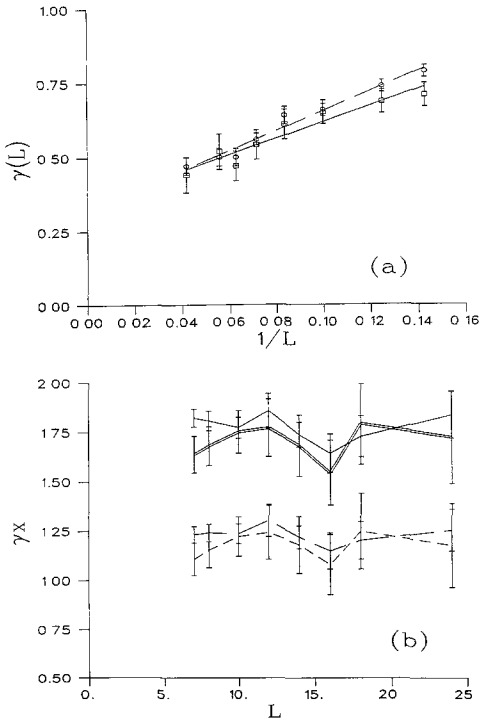

Fig. 3. (a) $\gamma(L)$ versus $1/L$. (○) Values obtained from $n(\ln(i))$. (□) Values obtained from $n(i)$. The lines show least-square fits with $\gamma(L) = m/L + \gamma_\infty$ and $\gamma_\infty(○) = 0.32 \pm 0.02$ and $\gamma_\infty(□) = 0.34 \pm 0.03$. (b) Plot of γx, with $x = L^{0.43}$, versus L for γ obtained from the logarithm-current distributions (single line), with $x = L^{0.43}$, for γ obtained from the current distributions (double line), with $x = 0.75 \ln(L)$, for γ obtained from the logarithm-current distributions (long-dash line), and, with $x = 0.75 \ln(L)$, versus L for γ obtained from the current distributions (short-dash line).

Similar graphs for different L values were obtained and we found that in this region we can write (see Fig. 3a)

$$n(\ln(i), L) = i^{\gamma(L)} \tag{5.2}$$

where γ is L dependent. For $L \to \infty$ we find $\gamma \to 0.33 \pm 0.06$.

In the region of small currents we can use Eq. (5.2) to obtain the current distribution $n(i)$ from the logarithm-current distribution $n(\ln(i))$

$$n(i) = n(\ln(i)) \frac{d(\ln(i))}{di} \sim i^{\gamma(L)-1} \tag{5.3}$$

From this we expect that $\ln(n(i))$ should be linear in $\ln(i)$ with a slope $\gamma - 1$. This is in fact observed in Fig. 2c for the cases $L = 10$ and $L = 18$. We can obtain $\gamma(L) - 1$ as the slope of $\ln(n(i))$ versus $\ln(i)$. Then we plot $\gamma(L)$ obtained in this way as a function of $1/L$ and by least squares fit obtain $\gamma_\infty = 0.34 \pm 0.03$ (see Fig. 3a). This is in agreement with the asymptotic value obtained by least squares fit from the logarithm-current distribution, namely $\gamma_\infty = 0.32 \pm 0.02$ (see Fig. 3a). We think that these error bars are too small. By visual inspection we conclude that $\gamma_\infty = 0.33 \pm 0.06$. From these plots it appears, however, that $\gamma(L)$ is not linear in L. In order to study the possibility that the logarithm-current distribution scales with $\ln i/\ln L$ as found in ref. 11, we plot in Fig. 3b both $\gamma(L) \cdot L^{0.43}$ and $\gamma(L) \cdot \ln(L)$ versus L, and find that they are both approximately constant. This indicates that we are considering a range of L values that is too narrow to differentiate between L scaling and $\ln L$ scaling, but that our results are not inconsistent with the latter.

Now we turn to a discussion of the moments. To obtain the exponents x_q and $\beta(q)$ of the moments of the current and logarithm-current distributions of Eqs. (1.3) and (1.5), we study the moments of the current and the logarithm-current distributions as a function of L and as a function of $\mathscr{L}$. We find that even though the values of x_q, β in finite samples do depend somewhat on whether L or $\mathscr{L}$ is used, their limits as $L \to \infty$ or $\mathscr{L} \to \infty$ are identical.

From Eq.(1.5) we get

$$\ln(\mathscr{M}_q) = \ln(B_q) + \beta(q) \ln[\ln(L)] \tag{5.4}$$

Here we have identified the point-to-point terminal distance $R = |x - x'|$ of Section 1 with the linear dimension L of Section 4.

The moments of the logarithm-current distribution divided by the number of bonds on the backbone $\mathscr{M}_q$ and the corresponding statistical errors for an applied potential difference between faces A and B are

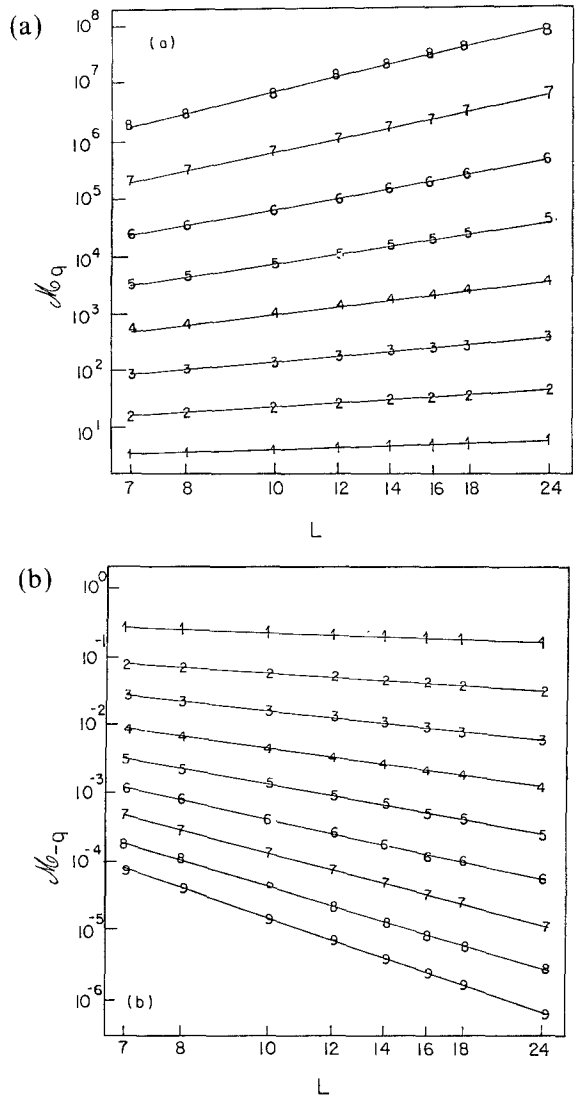

Fig. 4. (a) Positive moments of the logarithm-current distribution divided by the number of bonds on the backbone $\mathcal{M}_q$ versus $\ln[\ln(L)]$, for an applied potential difference between faces A and B. The numbers from 1 to 8 indicate the value of q. The straight-line fits of these moments by a least-squares algorithm are also shown. Error are not shown; see the text for a discussion of the errors. (b) Negative moments of the logarithm-current distribution divided by the number of bonds on the backbone $\mathcal{M}_{-q}$ versus $\ln[\ln(L)]$ for an applied potential difference between planes A and B. Numbers from 1 to 9 indicate the value of q. The statistical error at each point was smaller than the symbol used. The straight-line fits of these moments by a least-squares algorithm are also shown. (c) Plot of $\ln(B_q)$ ($\bigcirc$) and $\beta(q)$ ($+$) versus q for $-9 \leqslant q \leqslant 8$, as obtained from parts (a) and (b); see Eq. (1.5).

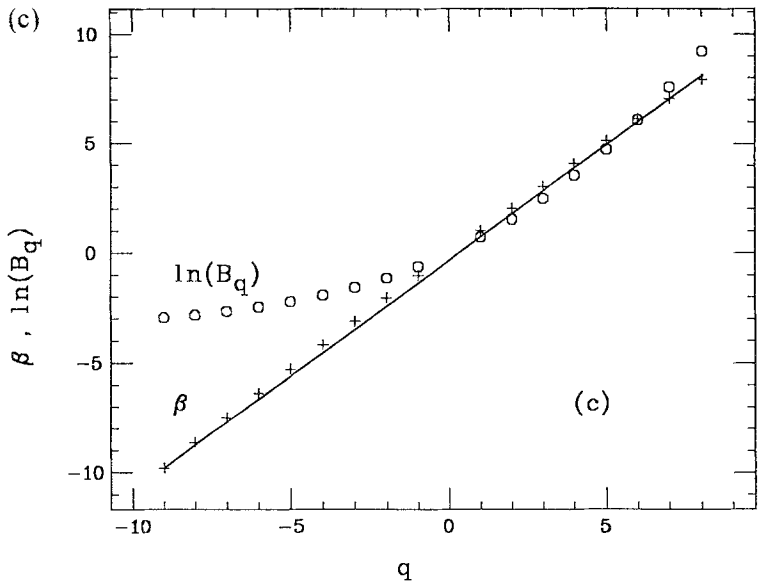

Fig. 4. (*Continued*)

exhibited as a function of $\ln(L)$ on a logarithmic scale in Fig. 4. A similar figure was obtained for an applied potential difference between face C and D. The positive moments are exhibited in Fig. 4a and the negative moments in Fig. 4b. The straight line fits of these moments to Eq. (5.4), using a least-squares algorithm, provide values for the amplitude B_q and the exponent $\beta(q)$. These lines are also shown in Figs. 4a and 4b. The estimated error bars were smaller than the symbols used. In Fig. 4c the values of $\beta(q)$ are exhibited versus q. A straight line of slope $c = 1.00 \pm 0.02$ gives a good fit at the positive values of q and some of the negative values. This is in agreement with results from hierarchical structures.[11]

The values of $\ln B_q$ are also exhibited in Fig. 4c. We find that these points can be fitted by

$$\ln(B_q) \sim q^{1.05} \qquad \text{for} \quad q \geqslant -3 \tag{5.5}$$

while

$$\ln(B_q) \sim |q|^{0.5} \qquad \text{for} \quad q \leqslant -3 \tag{5.6}$$

but this is clearly not the only possibility. In particular, it is possible to represent B_q by a simple exponential function $B_q \sim e^q$. Using this form, we get

$$\mathscr{M}_q \sim e^q (\ln L)^{cq} \sim (\log_{1.44} L)^{cq} \tag{5.7}$$

The moments of the logarithm-current distribution divided by the number of bonds on the backbone were also considered as a function of $\mathscr{L}$. Plots similar to Fig. 4 were obtained, but the numerical values of the slopes and amplitudes were somewhat different. We do not show these results here.

The fact that the results depend on the choice of the linear size considered (L or $\mathscr{L}$) is a finite-size effect. We are mainly interested in the asymptotic limit as $L \to \infty$, and in this case both calculations should converge to the same value. We therefore studied the local slope of Figs. 4a and 4b as a function of L. To minimize the effect of the large statistical error, we obtained the local slope from a least-squares fit of four consecutive points in Fig. 4 and its equivalent. The sum of the four L values that contribute to each point is denoted by n. Thus, for the first point, $n = 7 + 8 + 10 + 12 = 37$ (see Fig. 5).

In order to check the effect of replacing L by $\mathscr{L}$ as the linear size, we plot in Fig. 5 the local slope of the first moment of the logarithm-current distribution as a function of $1/n$ for both choices. In both limits $L \to \infty$ and $\mathscr{L} \to \infty$, we obtain by visual inspection $\beta(1) = 1.2 \pm 0.1$. A least squares fit gives 1.20 ± 0.05 in both cases, in agreement with out previous value, but with error bars that we think are too small. Evidently, using $\mathscr{L}$ instead of L, we get different results at each finite value of $\mathscr{L}$ or L, but the same value of $\beta(1)$ in the limit of infinite size (see Fig. 5). In contrast with this, the value of $\beta(1)$ we obtained from Fig. 4 was 1.00 ± 0.02 when we used L and 1.08 ± 0.02 when we used $\mathscr{L}$. The extrapolation procedure to infinite size

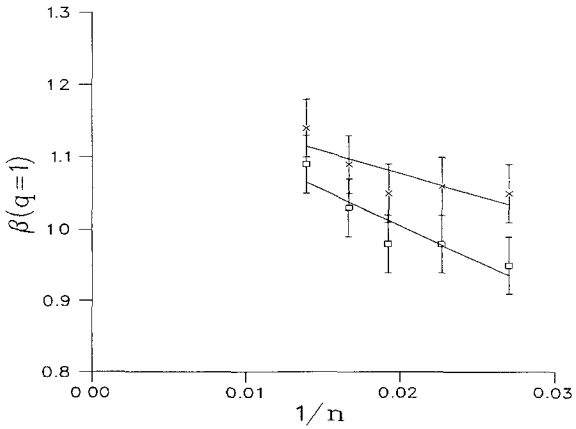

Fig. 5. Local slope of the first moment of the logarithm-current distribution $\beta(q = 1)$ versus $1/n$ when L (□) and $\mathscr{L}$ (×) are the considered linear dimensions; see Eq. (1.5). Least squares fits are also shown.

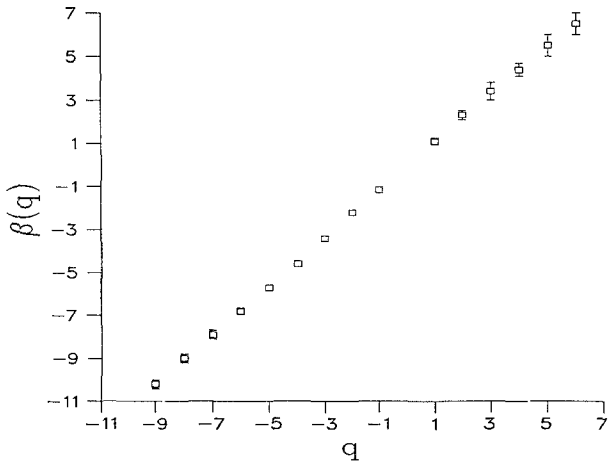

Fig. 6. Value of $\beta(q)$ as a function of q in the thermodynamic limit; see Eq. (1.5).

thus increases the value found for $\beta(1)$, and also renders it independent of the type of linear dimension used (L or $\mathscr{L}$).

The exponents $\beta(q)$ of the other positive and negative moments with their error were obtained by the same method of extrapolation (see Fig. 6). We then fitted the function $\beta(q)$ to the form cq with the result $c = 1.12 \pm 0.03$, When we restricted the fit to positive q we found $c = 1.06 \pm 0.10$.

The hierarchical models predict $c = 1$ for $q > 0$, which is inside the

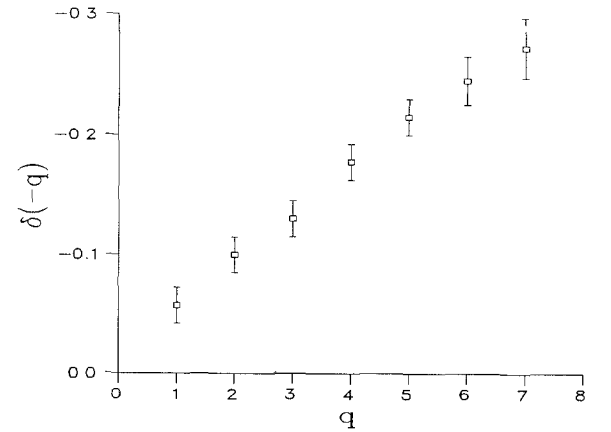

Fig. 7. Value of $\delta(-q)$ as a function of q in the thermodynamic limit; see Eq. (1.8).

error bars for the second value, but outside the error bars for the first values.

The value $c = 1.12 \pm 0.03$ obtained in the asymptotic limit is within the error bars of the value 1.06 ± 0.10 previously obtained, but it is larger than the hierarchical model predictions. This is mainly due to the values obtained for the negative moments, which have relatively small statistical errors. We also note that this value is obtained from the negative moments

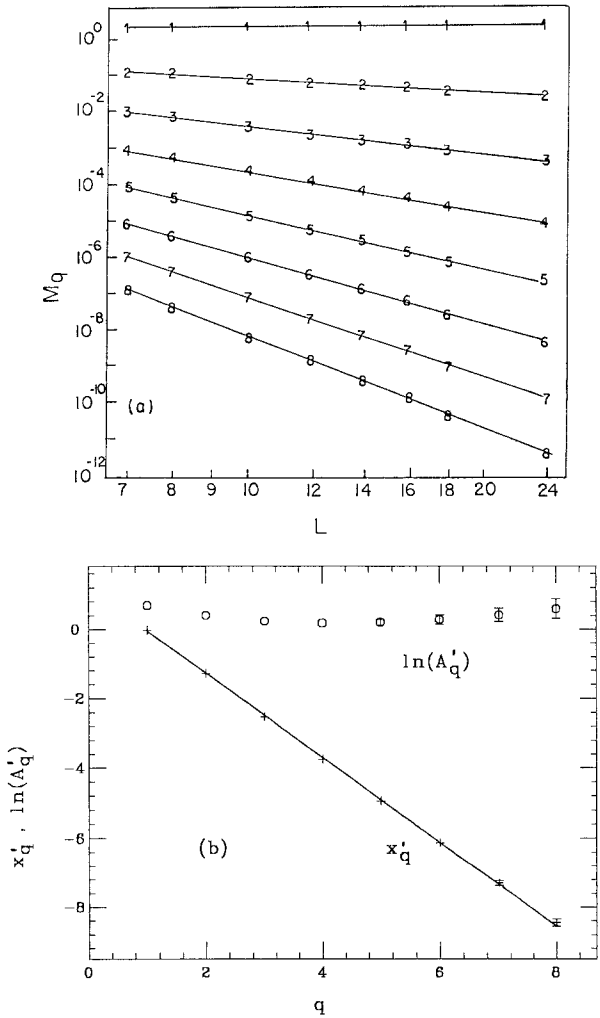

Fig. 8. (a) Positive moments of the current distribution M_q versus L on a logarithmic scale. The numbers from 1 to 8 indicate the value of q. The straight-line fits of these moments by a least-squares algorithm are also shown. (b) Plot of $\ln(A'_q)$ and x'_q versus q; see Eq. (1.3).

by assuming $\delta = 0$ in Eq. (1.8). This is done because our data are not good enough to simultaneously obtain both c and δ. However, we could fix c to the hierarchical model prediction ($c = 1$) and look for δ. To that end, we plot

$$\mathscr{M}_{-q}/\ln^{-q} L = L^{\delta} \tag{5.8}$$

as a function of L on a logarithmic scale. This yields $\delta(-q)$, which turns out to be L dependent. A local slope study similar to the one described before yields the asymptotic value of $\delta(-q)$ when $L \to \infty$. These values are exhibited in Fig. 7 as a function of q. We find that for for $c = 1$, $\delta(-q)$ depends on q and that for $1 < -q < 7$ it lies between zero and $1/\nu - D_b = -0.6$ as expected.[11]

We should emphasize that the value of c are obtained under the assumption that Eqs. (1.5) and (1.8) hold. Due to the small range of L values considered and to the relatively large error bars, we cannot distinguish between scaling as a function of $\ln L$ and scaling as function of L. That is, if we assumed $\mathscr{M}_q \sim L^{cq}$, $c = 0.42 \pm 0.003$ would be obtained.

In a similar way we studied the moments of the current distributions. The moments M_q of the current distributions and the corresponding statistical error are shown as a function of L in Fig. 8a on a logarithmic scale. The straight-line fits of these moments by a least-squares algorithm provide the amplitude A'_q and the exponent x'_q of Eq. (1.3) along with error bars. These results are shown in Fig. 8b. The value of $\ln(A'_q)$ appears to be nearly independent[22] of q. Simulations at larger L's should be done to confirm this behavior.

The moments of the current distributions were also plotted versus $\mathscr{L}$, and straight lines fitted. Plots similar to Fig. 8 were obtained, but the numerical values of the slope and amplitude were slightly different. To save space, we omit those figures here.

Table I. Exponents of the Moments of the Current Distributions

q	x'_q	x_q	ψ_q	Prediction[5]
1	-0.03 ± 0.02	1.26 ± 0.03	1.12 ± 0.03	
2	-1.29 ± 0.02	1.29 ± 0.04	1.14 ± 0.04	1.12 ± 0.02
3	-2.55 ± 0.04	1.32 ± 0.07	1.17 ± 0.07	
4	-3.80 ± 0.07	1.36 ± 0.10	1.20 ± 0.10	1.05 ± 0.03
5	-5.10 ± 0.06	1.35 ± 0.10	1.20 ± 0.10	
6	-6.50 ± 0.05	1.24 ± 0.13	1.09 ± 0.13	1.02 ± 0.03
7	-7.6 ± 0.1	1.40 ± 0.20	1.27 ± 0.20	
8	-8.9 ± 0.1	1.40 ± 0.20	1.26 ± 0.20	1.01 ± 0.03

These slopes were analyzed as in the case of the logarithm-current distribution and the results are shown in Table I. We include in this table the values of x'_q, $x_q = x'_q - qx'_2$, $\psi_q = \nu x_q$ (with[23] $\nu = 0.89 \pm 0.01$) and the predictions of ref. 5. The values of ψ_q we obtained are in agreement with those predictions. The value of $b = \psi_4 = 1.36 \pm 0.10$ is also in agreement with known bounds[9] and previous simulation results.[7,8]

6. CONCLUSIONS

We have shown that below some critical current, the logarithm-current distribution in three-dimensional random-resistor networks at the percolation threshold increases as i^γ with an asymptotic value $\gamma = 0.33 \pm 0.06$ when $L \to \infty$. A further study of the L dependence of γ shows that the logarithm-current distribution may scale with $\ln(i)/\ln(L)$. These new results regarding power law i^γ do not follow in any simple way from the behavior of the moments of either $\ln i$ or i, which were investigated in the past. They were discovered only as a result of a study of the actual distribution function.

We found that a careful consideration of the roundoff errors is very important in the study of the logarithm-current distribution. We were able to study this distribution by applying a modified transfer matrix method for simulating random resistor networks and properly eliminating the spurious currents which appeared in the dangling ends. We find that c is probably between 1 and 1.15, and that δ may be a function of q. These calculations show that the hierarchical model result is close to the true value. Simulations done on the backbone only, by first eliminating the dangling clusters, are necessary to further check the hierarchical model predictions.

ACKNOWLEDGMENTS

We would like to thank the authors of ref. 11, especially RB, for useful discussions and for bringing to our attention preliminary results from their calculations. This research was supported in part by the U.S.–Israel Binational Science Foundation under grant 354/85 and by the Israel National Center for Absorption in Science.

REFERENCES

1. R. Rammal, C. Tannous, and A. M. S. Tremblay, *Phys. Rev. A* **31**:2662 (1985).
2. R. Rammal, C. Tannous, P. Breton, and A. M. S. Tremblay, *Phys. Rev. Lett.* **54**:1718 (1985).
3. L. de Arcangelis, S. Redner, and A. Coniglio, *Phys. Rev. B* **31**:4725 (1985).

4. L. de Arcangelis, S. Redner, and A. Coniglio, *Phys. Rev. B* **34**:4656 (1986).
5. R. Blumenfeld, Y. Meir, A. Aharony, and A. B. Harris, *Phys. Rev. B* **35**:3524 (1987).
6. Y. Park, A. B. Harris, and T. C. Lubensky, *Phys. Rev. B* **35**:5048 (1987).
7. I. Balberg, N. Wagner, D. W. Hearn, and J. A. Ventura, *Phys. Rev. B* **37**:3829 (1988).
8. A. Kolek and A. Kusy, *J. Phys. C* **21**:L573 (1988).
9. D. C. Wright, D. J. Bergman, and Y. Kantor, *Phys. Rev. B* **33**:396 (1986).
10. A. M. S. Tremblay, S. Feng, and P. Breton, *Phys. Rev. B* **33**:2077 (1986).
11. J. Adler, R. Blumenfeld, Y. Meir, A. Aharony, and A. B. Harris, private communication.
12. D. J. Bergman, E. Duering, and M. Murat, *J. Stat. Phys.* **58**:1 (1990).
13. B. Fourcade and A. M. S. Tremblay, *Phys. Rev. A* **36**:2352 (1987).
14. G. G. Batrouni, A. Hansen, and M. Nelkin, *J. Phys.* (Paris) **48**:771 (1987).
15. J. P. Straley, *Phys. Rev. B* **39**:4531 (1989).
16. S. Wilke, *Phys. Lett. A* **96**:344 (1983).
17. B. Derrida and J. Vannimenus, *J. Phys. A* **15**:L557 (1982).
18. J. Hoshen and R. Kopelman, *Phys. Rev. B* **14**:3438 (1976).
19. H. J. Herrmann, D. C. Hong, and H. E. Stanley, *J. Phys. A* **17**:L261 (1984).
20. G. R. Jerauld, L. E. Scriven, and H. T. Davis, *J. Phys. C* **17**:3429 (1984).
21. B. Derrida, D. Stauffer, H. J. Herrmann, and J. Vannimenus, *J. Phys.* (Paris) **44**:L701 (1983).
22. B. Fourcade, P. Breton, and A. M. S. Tremblay, *Phys. Rev. B* **36**:8925 (1987).
23. D. W. Heermann and D. Stauffer, *Z. Phys. B* **44**:339 (1981).